The Au-Cu bimental catalyst by renewable γ-Al_2O_3 as supports for acetylene hydrochlorination

Jigang ZHAO[1,*], Junjian ZENG[1], XiaoguangCHENG[1], Lei WANG[1,2], Henghua YANG[1], Benxian SHEN[1]

[a]*State Key Laboratory of Chemical Engineering, East China University of Science and Technology, 130 Meilong road, Shanghai 200237, PR China;*

[b]*TianjinDagu Chemical Co., Ltd., 1 Xinghua Road, Tianjin 300455, PR China*

* Corresponding author. Tel.: +86 21 64252916; fax: +86 21 64252851

E-mail address: zjg@ecust.edu.cn (J.G Zhao)

Characterization

XRD data was collected using a Bruker D8 advanced X-ray diffract meter with Cu-Kα irradiation at 40 kV and 40 mA in the scanning range of 10° and 80°. H_2-TPR was performed using a Micromeritic ASAP 2920 instrument, using 10% H_2 in argon (flow 50 ml/min) as a reductive gas and a temperature ramp of 50 to 600 ℃(ramp rate, 10 ℃/min) with the TCD detector recording the signal. Metal content analysis using Varian's 710ES inductively coupled plasma atomic emission spectrometry (ICP-AES) measurement instrument. Plasma gas flow rate of 15 ml/min, atomizing air pressure 200 kPa.

Result and discussion

The actual loading amount of active component

Table.1S ICP-AES results of $AuCl_3$-$CuCl_2$/Al_2O_3 samples before and after used

Samples	Cu, wt%	loss ratio, %	Au, wt%	loss ratio, %
Fresh sample	1. 37	8.76	0.10	10.00
Deactivated sample	1.25		0.09	

Structure and textural properties

The profiles were similar and showed broad peaks belonging to the faces (3 1 1), (4 0 0) and (4 4 0) of the γ-Al_2O_3 phase (JCPDS card No. 43-1308), which indicated that all the supports have similar crystal structure.

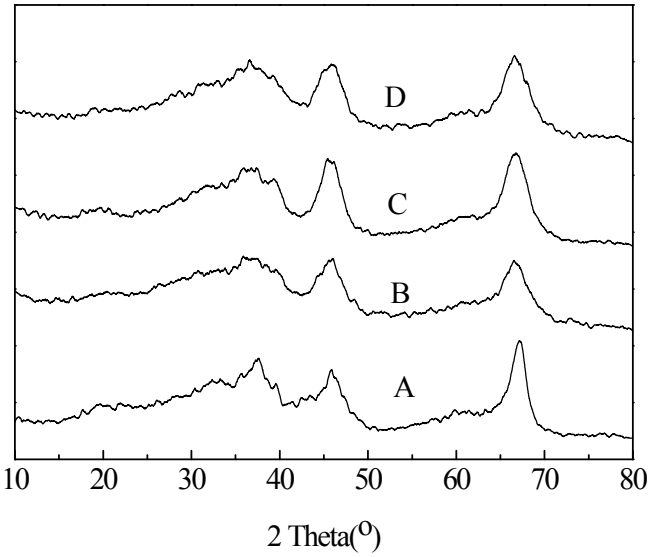

Fig. S1 XRD patterns of sample A, B, C and D.

The nitrogen adsorption desorption isotherms of four γ-Al_2O_3 are illustrated in Fig. S2a. In all cases, the isotherms were ascribed to the type IV according to the IUPAC classification, which were produced by the mesoporous materials. A typical feature could be observed that a hysteresis loop and a platform in a region of higher p/p^0

values, sometimes ended with isotherm eventually turned up. The isotherms of sample A and D exhibited an hysteresis loop intermediate between H2 and H4 (IUPAC classification) due to open tubular pores with circular or polygonal sections and a pore size distribution with a maximum frequencies of pore diameters between 6 and 20 nm (Fig.S2b). The isotherm of sample B and C, which had a similar hysteresis loop, could be classified as type H2. The pores showed a smaller pore size distribution than sample A and D.

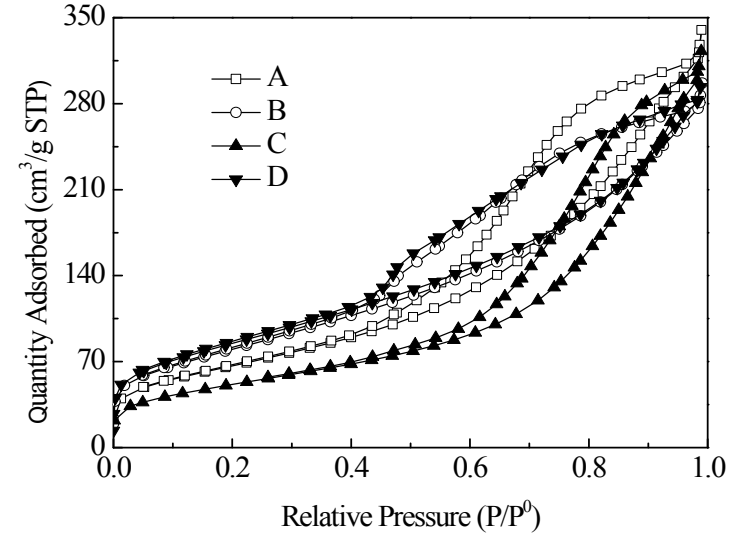

(a)

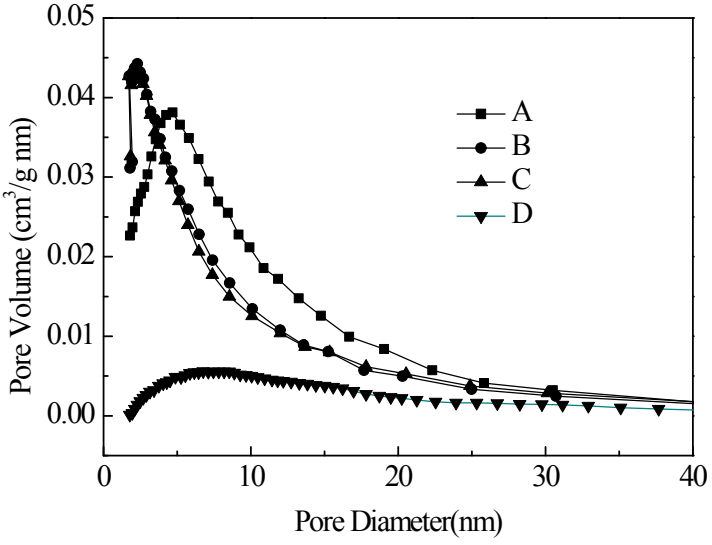

(b)

Fig. S2 Porosity profiles (a) Nitrogen adsorption–desorption isotherms; (b) pore size

distribution.

Possible mechanism for the influence of the base site to the activity

H_2-TPR analysis provided some evidence that the base site of the Al_2O_3 support played an important role in the dispersion of the Au^{3+}. Nkosi[1, 2] had confirmed that Au^{3+} is the main activity site in the acetylene hydrochlorination. H_2-TPR profiles for fresh catalysts are shown in Fig. 5. The reductive peak at approximately 228 ℃ was attributed to the reduction of Au^{3+} to Au^0. Compared with ACAlD, the others had different degree of forward migration of peak which was due to the relative poorer dispersion of the active ingredient Au^{3+}, and it was consistent with their catalyst activity. The second reductive peak at approximately 330 ℃ was attributed to the reduction of Cu^{2+} to Cu^0. It was obvious that they also have migration phenomenon, just as the Au^{3+}.

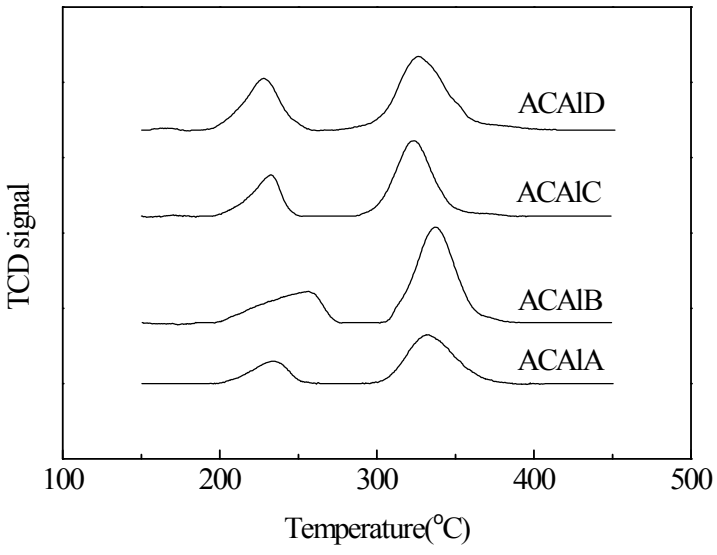

Fig. S3 H_2-TPR profiles of $AuCl_3$-$CuCl_2$ supported on γ-Al_2O_3.

TEM

The TEM images of fresh catalysts were shown in Fig. 6. No significant highly

metal dispersion was observed in ACAlA and ACAlB, which attributed to areunion phenomenon for the activity metal. To the fresh ACAlC, ACAlD, small black dots appeared on the substrate, they were dispersed Au particles. It indicated more obvious aggregation of Au particles associated with surface groups, which showed a positive relationship between the metal dispersion and the catalysis activity, which was consistent with the TPR results.

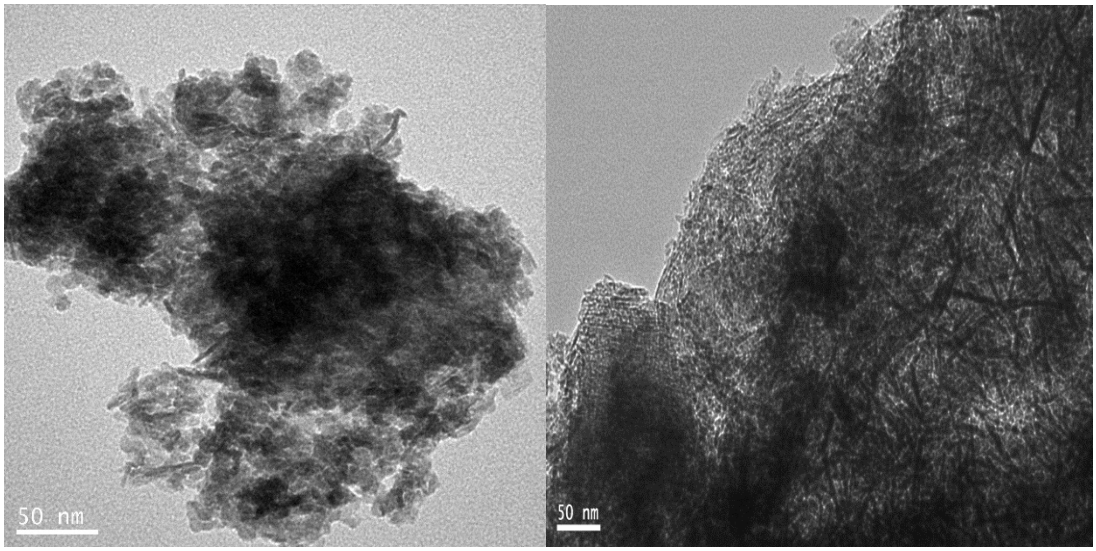

(a) (b)

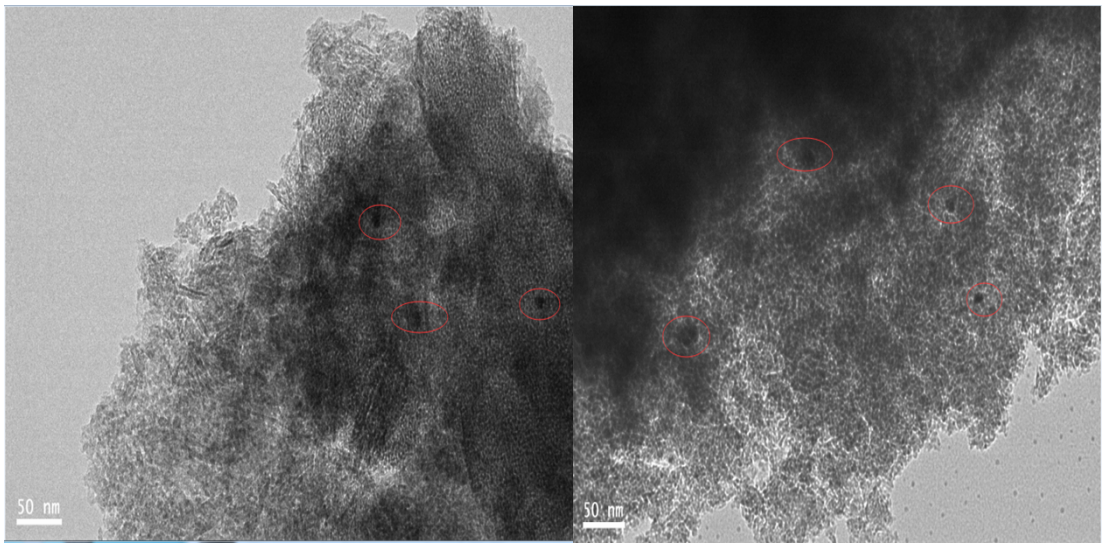

(c) (d)

Fig. S4 TEM images of fresh catalyst (a) ACAlA;(b)ACAlB;(c)ACAlC;(d)ACAlD.

Schematic plot

The possible mechanism sketch for the enhanced stability and catalytic efficiency was shown in Fig. S5

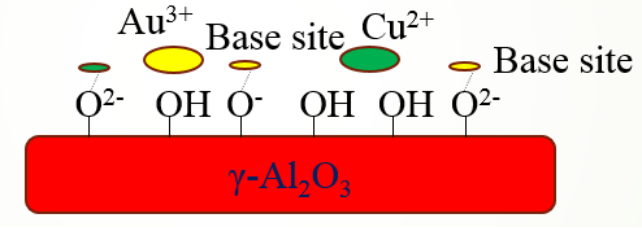

Fig. S5 The possible mechanism sketch.

The support modification initially by potassium hydroxide

The CO_2-TPD profile of MB was shown in Fig. S6, it can be seen that an obvious strong base site appeared.

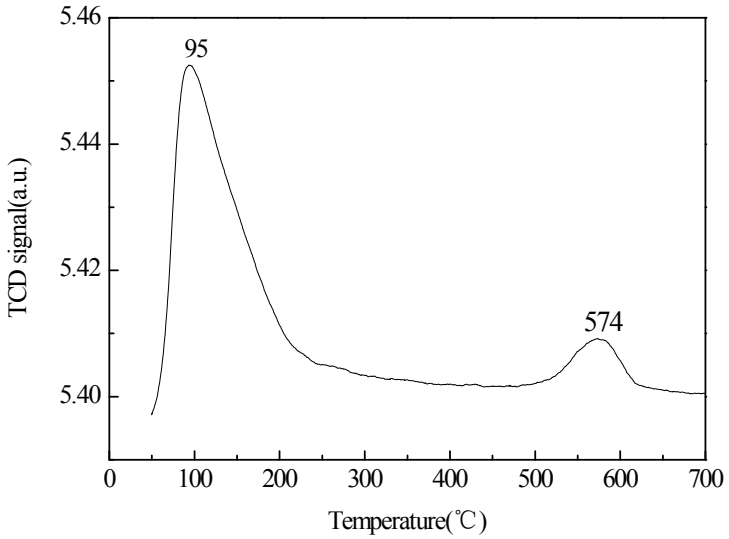

Fig. S6 CO_2-TPD profile of MB.

Reference

[1] B. Nkosi, M. D. Adams, N. J. Coville, G. J. Hutchings, *J. Catal.*, 1991, **128**, 378-

386.

[2] B. Nkosi, N. J. Coville, G. J. Hutchings, *Appl. Catal*., 1988, **43**, 33-39.

[3] M. Conte, A. F. Carley, G. Attard, A. A. Herzing, C.J. Kiely, G. J. Hutchings, *J. Catal.*, 2008, **257**, 190-198.